

Study of Mechanical and Physicochemical Properties of Polycrystalline Alumina Implanted with Titanium

F. Halitim,^a S. Paletto,^a G. Fantozzi^a & D. Treheux^b

^a INSA-GEMPPM, URA 341, 69621 Villeurbanne, France

^b ECL — Départ Matériaux Mécanique Physique Ecully, France 69631

(Received 10 June 1994; revised version received 21 February 1995; accepted 10 March 1995)

Abstract

A study of ion implantation in polycrystalline alumina has been undertaken aimed at two principal areas. Firstly the measurement of the evolution of mechanical properties in the treated surface, such as hardness and fracture toughness, was undertaken using a Vickers indentation method. These properties are very sensitive to the presence of residual stresses and to the surface microstructure. Secondly a physicochemical study of the treated surface using XRD and SEM techniques in order to identify the parameters that influence the mechanical changes was undertaken.

1 Introduction

The thermomechanical properties of structural ceramics depend strongly on their surface state: e.g. fracture in brittle materials is frequently due to the flaws present on the surface. Ion implantation is one of the methods currently used to overcome this difficulty, since the method has the advantage that the net shape and dimensions of the samples are preserved even after the treatment. Most of the studies on ion implantation up to now have been carried out on single crystals.^{1–3} We report here on a study of ion implanted polycrystalline alumina. In the case of ion implantation with zirconium, an element which readily oxidises to ZrO₂, which is not miscible in alumina, the formation of a zirconia reinforced alumina composite layer has been observed.⁴ It is therefore equally interesting to study the case of titanium implantation in alumina since titanium also oxidises very easily to TiO₂ which has considerable solubility in alumina.⁵ Earlier studies on the ion implantation of Ti⁺ and Y⁺ ions in single crystals has revealed that compressive stresses are created in the implanted zone.⁶ These stresses provide a possibility of reducing the spreading of radial cracks on the

sample surface, which leads to variations in the surface mechanical properties. It is also possible under certain conditions, to form an amorphous surface layer by this technique. In the case of titanium implantation into sapphire, the amorphous layer is not formed until the fluence is less than 10¹⁷ ions/cm² (at room temperature) or until the temperature is lowered to 77 K with smaller doses.⁷ The microstructure of the implanted zone depends generally on the fluence level and the ion energy, as well as on the temperature of implantation, the nature of the ion implanted and the state of the substrate surface.⁸ A post-thermal treatment could allow the possibility of other changes in the microstructure and in the phases present in the implanted layer which, in turn, could lead to changes in the mechanical properties. It is therefore necessary to understand the processes that follow the thermal treatment of the ion implanted layers.

2 Experimental

2.1 Sample preparation

Polycrystalline alumina samples (MATROC D995 F) of 99.95% purity and a grain size <3 µm was used in this study. The samples were polished rigorously to the same reference level (fixed roughness).

Polishing grinding

The samples were ground to levels of assured planarity by fixing them on rotating metallic disks and using a diamond paste of 6 µm size for a period of about 20 min under a pressure of 1 bar.

Polishing

Final polishing was done on a felt disc using polycrystalline diamond paste of 3 µm, followed by a diamond paste of 1 µm, the different operations led to a surface roughness < 0.02 µm. To reduce the damages induced by polishing, the samples were post annealed in air for 1 h at 1200°C.

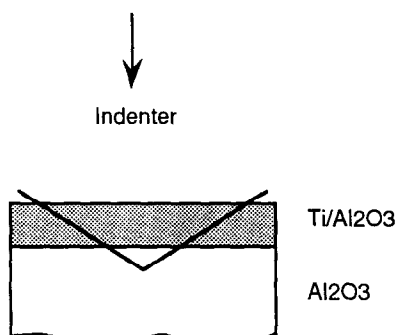


Fig. 1. Indenter into the implanted layer.

2.2 Ion implantation

Ion implantation was conducted using mono-charged ions produced by an isotopic separator which permits separation of mono-charged ions possessing a maximum energy of 110 Kev; doses of 2×10^{16} ions/cm² and 10^{17} ions/cm² are used in this study. The higher dose is the limit, for this energy, to obtain an implanted layer without amorphisation.⁷ During the implantation, the temperature of the target was maintained at the ambient level using a water circulation system for the target holder. After implantation, thermal treatment at three different temperatures 1000, 1200 and 1500°C was conducted for 1 h in air in all cases.

2.3 Vickers hardness

The hardness of the implanted alumina samples was obtained by the ratio of the load to the surface contact area. The Vickers microhardness was measured on a non-instrumented microhardness tester (WOLPERT VTD 11 Type) using loads in the range of 0.1–10 N. The loads were applied to the sample for a period of 30 s in all cases. The unit was fitted with an optical system with two scales of magnification. The samples were subjected to 10 indentations under different loads (0.1, 0.25, 0.5, 1, 2, 3, 5 and 10 N). For the smallest load, the indents were of the order of 3 µm, thus we are unable to observe them accurately. Hence an indirect method has been used, where an optical microscope with its immersion objective attached camera with a high resolution film is used. This permits a magnification of 10 000 and increases the possibility of measuring such small indents, without, however, increasing the resolving power of the microscope. The photography enables us to measure the indents with a higher definition (a few %). The implanted layer is about 1000 Å thick and the lowest charge of 0.1 N was used for the indentation, shown schematically in Fig. 1. As stated above, this arrangement indicates the direction of the changes in the hardness value, but not the exact value of the hardness of the implanted layer.

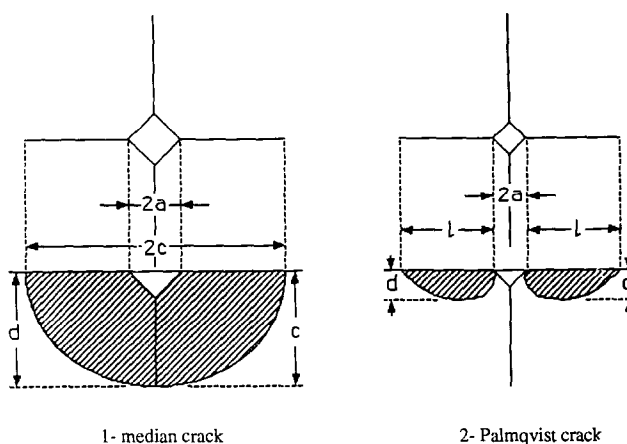


Fig. 2. Crack system.

If the hardness of the implanted layer increases this increases the measured hardness as well.

2.4 Fracture toughness

The Vickers indentation is particularly suitable to measure the toughness of brittle materials. Recently Liang *et al.*⁹ have proposed a unified formula which enables the determination of toughness in both cases of median or Palmqvist's cracks, shown schematically in Figs 2.1 and 2.2.

$$\frac{K_{IC}\Phi}{Ha^{1/2}} \left(\frac{H}{E\Phi} \right)^{0.4} \alpha = \left(\frac{c}{a} \right)^{(c/18a) - 1.51}$$

$$\alpha = 14 \left[1.8 \left(\frac{4\nu - 0.5}{1 + \nu} \right)^4 \right]$$

where a and c are respectively: the semidiagonal length of indent and the half length of the cracks produced by indentation. Φ is a constant ≈ 3 , ν is Poisson's ratio, H the hardness and E the Young's modulus of the material. The load at which the crack is initiated is 2 N. A knowledge of the length of the crack, $2c$, and the hardness of the material, H , would enable the determination of toughness K_{IC} . The polycrystalline material used in this study is an industrial product and possesses a heterogeneous microstructure; this leads to a

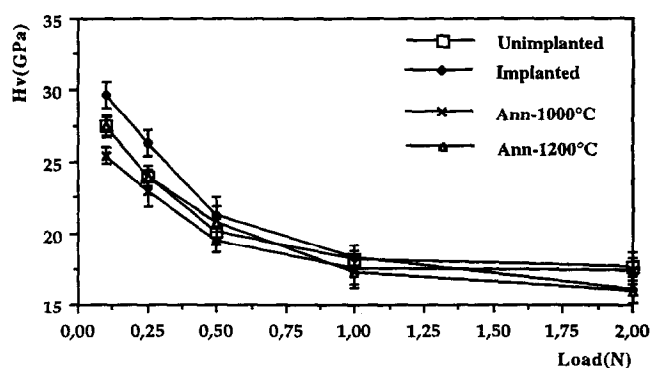


Fig. 3. H_v versus load in Ti^+ implanted Al_2O_3 , dose 2×10^{16} ions/cm².

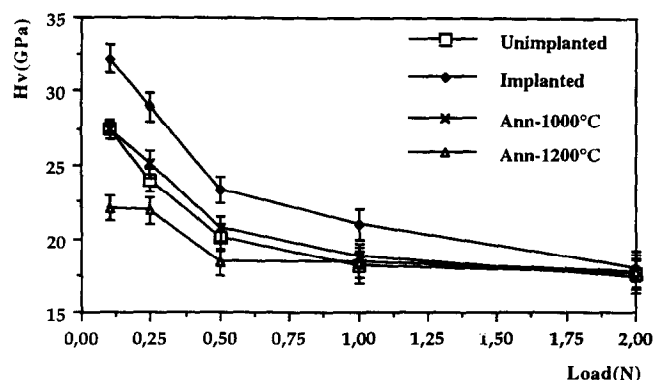


Fig. 4. H_v versus load in Ti^+ implanted Al_2O_3 , dose 10^{17} ions/ cm^2 .

dispersion in the measured values of toughness. For this reason, the results showing a large deviation from the mean values are excluded in this study. The mean values derived give an indication of the changes to the material toughness.

3 Experimental Results

3.1 Hardness

The curves of Figs 3 and 4 present the variation of hardness as a function of the load used for different temperatures of annealing and for the two implantation doses mentioned. As stated earlier, the most significant values of hardness are obtained at a load of 0.1 N.

3.2 Toughness

Figures 5 and 6 present the evolution of toughness as a function of load and the temperature of annealing. Cracks occur only after a particular applied load. The K_{IC} values have been calculated for different loads.

3.3 Physicochemical analyses

Figure 7 presents the evolution of the superficial microstructure observed in a scanning microscope at the two implantation dose levels and for different temperatures of annealing. (Fig. 7(a–d)) for the

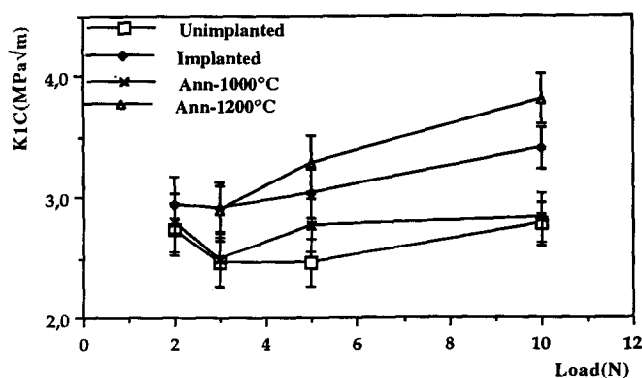


Fig. 5. Variation of K_{IC} as a function of applied load on Ti^+ implanted Al_2O_3 , dose 2×10^{16} ions/ cm^2 .

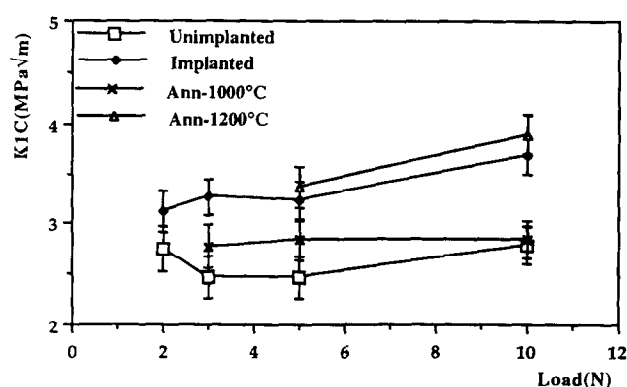


Fig. 6. Variation of K_{IC} as a function of applied load on Ti^+ implanted Al_2O_3 , dose 10^{17} ions/ cm^2 .

dose 2×10^{16} ions/ cm^2 and Fig. 7(e–h) for the dose 10^{17} ions/ cm^2 respectively).

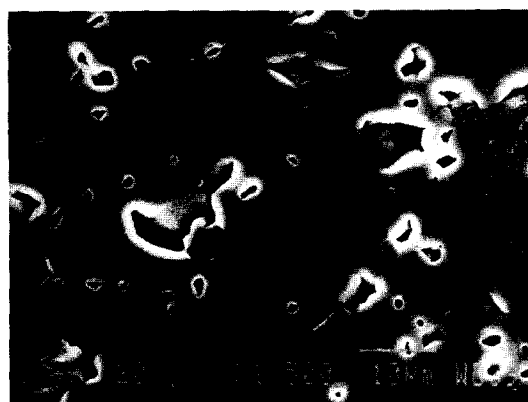
It can be seen that for the unannealed samples the surface is free of precipitates, (Fig. 7(a–e)). These precipitates only appear at 1000°C and grow at 1200°C , (Fig. 7(c–g)). Annealing at 1500°C removes the precipitates so that only the grain boundaries remain, (Fig. 7(d–h)).

Figure 8 presents the X-ray diffraction diagrams at grazing incidence (GXR) obtained for the implanted sample (Fig. 8(a)) for both doses of 2×10^{16} ions/ cm^2 and 10^{17} ions/ cm^2 annealed at 1000°C and Fig. 8(b) for both doses of 2×10^{16} ions/ cm^2 and 10^{17} ions/ cm^2 annealed at 1200°C respectively). The peaks without indices correspond to $\alpha\text{-Al}_2\text{O}_3$ and the others indicate the presence of the tetragonal TiO_2 obtained after annealing.

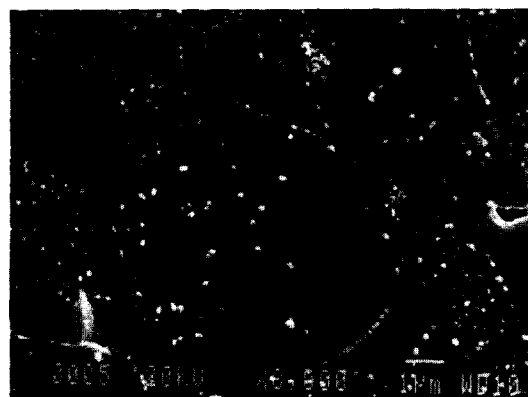
4 Discussion of the Results

The result of titanium implantation into polycrystalline alumina is an enhancement of the hardness of 8 and 18% for dose levels of 2×10^{16} ions/ cm^2 and 10^{17} ions/ cm^2 respectively. When the implanted samples are thermally annealed at 1000°C , the hardness was found to decrease for both doses. However, while thermal annealing at 1200°C recovers the hardness value to that of the unimplanted alumina in the case of the smaller dose, the hardness value lies much below that of the unimplanted alumina in the case of the higher dose. It should be noted also that changes in the toughness K_{IC} in the case of both doses follow a trend similar to the case of hardness (Fig. 6).

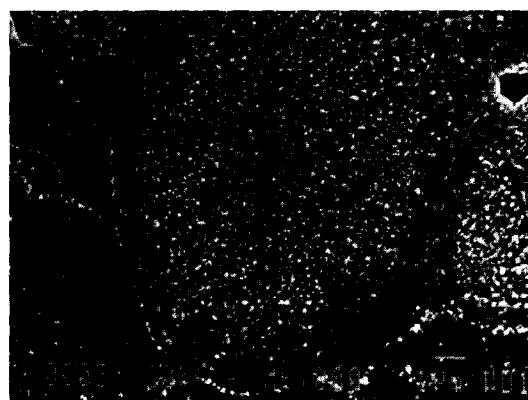
An appreciable increase in the value of K_{IC} could be noticed in the case of both doses (22% for the smaller dose and 32% for the larger dose). Thermal annealing at 1000°C lowers the values of K_{IC} in both cases while thermal annealing at 1200°C finally leads to an increase in the value of toughness (32 and 40% for the small and the high doses respectively).



(a)-unannealed



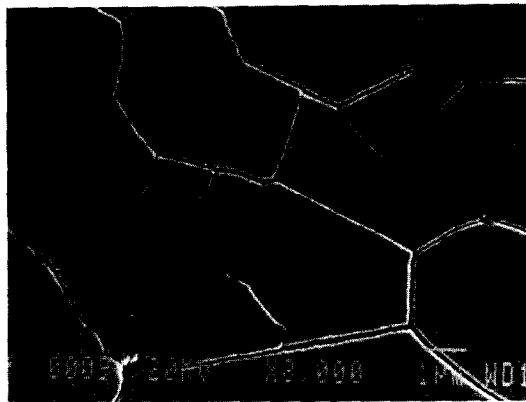
(b)-1000°C



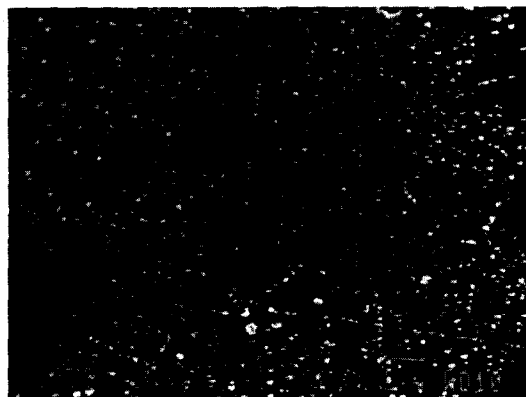
(c)-1200°C



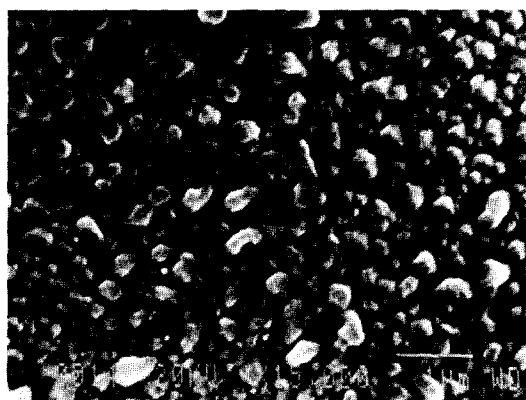
(d)-1500°C



(e)-unannealed



(f)-1000°C



(g)-1500°C



(h)-1500°C

Fig. 7. Microstructure of the implanted alumina before and after annealing at different temperatures: a-d — dose: 2×10^{16} ions/cm² and e-h — dose: 10^{17} ions/cm².

The scanning electron microscopic (SEM) studies show that the microstructure of all the implanted alumina samples is similar and the porosities present in alumina are visible (Fig. 7(a)–(b)). Thermal annealing at 1000°C creates precipitates in the grain and on the grain boundaries (Fig. 7(b)). Annealing at 1200°C increases the quantity of precipitates which have a size less than 1 μm (Fig 7(c–g)). At 1500°C, the precipitates disappear and only the grains remain visible (Figs 7(d–h)) the surface becomes irregular and measurement of the indent or cracks dimensions is no longer possible. It is also observed that implantation at the larger dose leads to rupture of the grain boundaries (Fig. 7(e)) as an increase in the size and number of precipitates at the lower dose level (Fig. 7(f–h)).¹⁰

The principle of X-ray diffraction at grazing incidence is the same as for classical X-ray diffraction studies. The X-ray beams of constant intensity fall on the sample under grazing incidence

(a few tenths of 1 or 2 degrees). The penetration of X-ray beams is a function of this angle and the depth of analysis is variable. These diagrams reveal the presence of TiO_2 at 1000 and 1200°C (Fig. 8(a–b)) for both doses. At room temperature and at 1500°C the XRD reveals only the presence of $\alpha\text{-Al}_2\text{O}_3$. These X-ray diffraction studies show that the oxidation of titanium occurs during the heat treatment and may be due to the oxygen ions displaced from the substrate by the ion implantation, or an external ingress of oxygen.¹¹

On the basis of the XRD and SEM studies, these results can be explained in the following manner:

- (i) For the two doses used, the increase of hardness observed on the implanted samples which remain crystalline,¹² could be attributed to the compressive stresses induced by implantation.
- (ii) When the annealing temperature is increased, two phenomena are induced simultaneously, namely stress relaxation and TiO_2 formation.

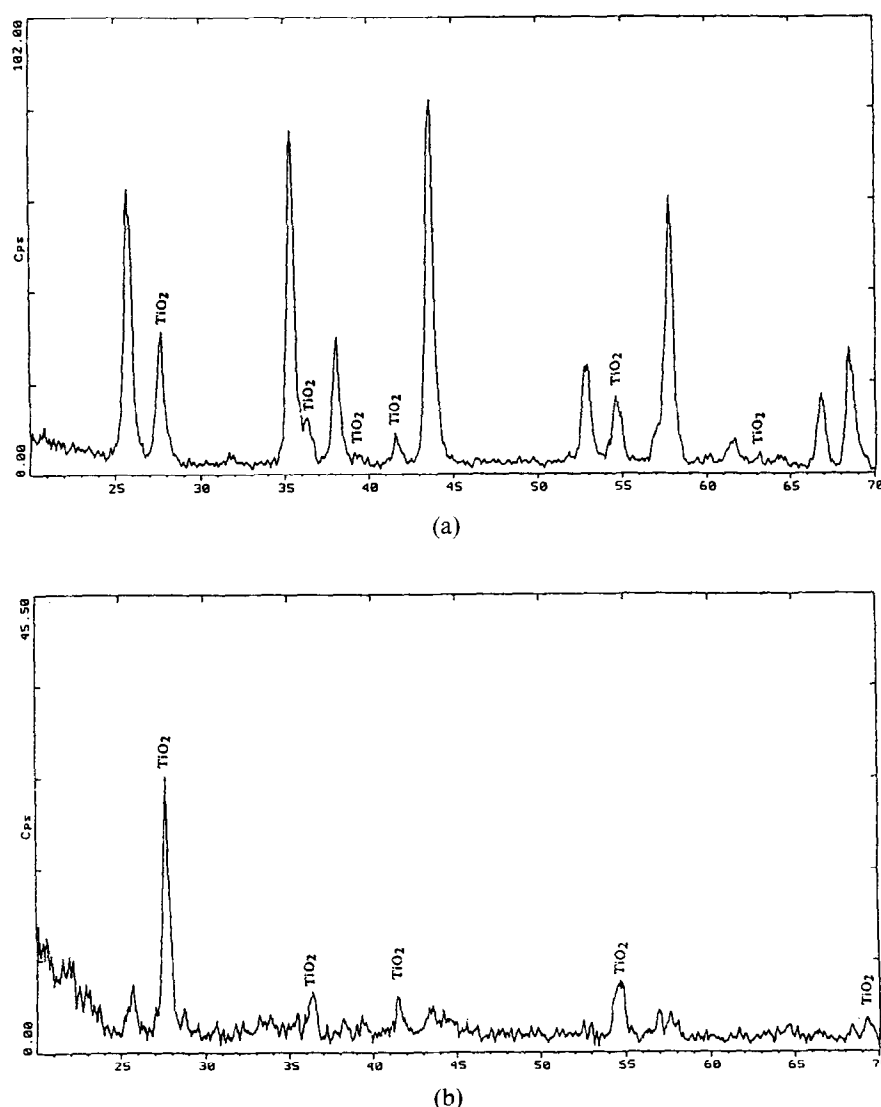


Fig. 8. GXR D patterns showing the effect of annealing for ion implanted alumina. (a) Doses 2×10^{16} ions/ cm^2 and 10^{17} ions/ cm^2 , annealed at 1000°C, ($\alpha = 0.3^\circ$). (b) Doses 2×10^{16} ions/ cm^2 and 10^{17} ions/ cm^2 , annealed at 1200°C, ($\alpha = 0.5^\circ$).

One can see that for implantation at the 2×10^{16} ions/cm² dose followed by thermal annealing at 1200°C there is very little formation of TiO₂ and the initial hardness of the unimplanted sample is recovered. For the 10^{17} ions/cm² dose, the hardness obtained is much less since there is an appreciable formation of TiO₂, whose hardness is less than that of pure alumina. At a temperature which is close to the sintering temperature of alumina (1500°C), the implanted ions are entirely ejected from the implanted surface.

According to Burnett and Page,⁶ the residual stresses introduced in the implanted layer are compressive in nature. These stresses were observed by the beam embedding of thin samples method,¹³ and also by the measurement of variation of the radial crack length around the Vickers indent. Lawn and Fuller¹⁴ have given a relationship which gives the values of these stresses.

$$1 - \left(\frac{C_0}{C} \right)^{3/2} = \frac{2\Psi\sigma_s d^{1/2}}{K_c}$$

where K_c is the substrate toughness, C_0 is the radial crack length at $\sigma_s = 0$, C is the crack length at stress σ_s , and Ψ is a constant taken as unity ($= 1$). In the case where $C < C_0$, σ_s is negative, and the stresses are compressive. The following tables show the values of σ_s (residual stress) obtained for three values of the crack length.

The results obtained with different indentation loads give slightly different values of stress. The method of Lawn and Fuller gives lower values of stress than the method of Krefit and Eernisse.¹⁵

Generally, implanted samples become amorphous and this leads to the enhancement of the toughness,¹⁰ but the fluences used in this study are not sufficient to amorphise alumina.⁶ Hence, we should consider again the idea developed here that the toughness increase for the as-implanted samples is due to the compressive stresses induced by the implantation.

Annealing at 1000°C relaxes these stresses and we obtain a value of toughness close to that of unimplanted alumina. At 1200°C, there is a formation of TiO₂ which gives a toughness value higher than that of alumina. In particular the case where a load of 5 N has been applied, (Figs 5 and 6) an enhancement of 32% for the dose of 2×10^{16} ions/cm² and of 36% for the dose of 10^{17} ions/cm² is observed. We propose that the residual stresses increase with the implanted dose. This could be attributed to a large concentration of induced defects, point defects and dislocations.¹⁰

Figure 9 shows a schematic representation of the evolution of the implanted layer composition as a function of annealing temperature and a pictorial representation of the results obtained in the SEM studies.

Table 1. Values of σ_s obtained for the two doses. (a) 2×10^{16} ions/cm². (b) 10^{17} ions/cm²

Load (N)	10 (N)	5 (N)	3 (N)
Co (μm)	84	54	38
C (μm)	72	48	34
σ_s (MPa)	-1040	-800	-770

(a)

Load (N)	10 (N)	5 (N)	3 (N)
Co (μm)	83	54	38
C (μm)	68	43	31
σ_s (MPa)	-1534	-1638	-1422

(b)

5 Conclusion

The surface mechanical properties of ceramics could be modified by ion implantation. Such modifications are a result of the change in material microstructure and in the residual stresses produced in the implanted layer.

The specific case of Ti⁺ ions implanted in polycrystalline alumina is studied here at 2×10^{16} and 10^{17} ions/cm², an increase in hardness due to the effect of compressive stresses is noted at room temperature. These stresses relax with the formation of a layer of TiO₂ when implanted samples are annealed at 1000°C, leading to a decrease of the sample hardness. However, this relaxation effect is compensated by the formation of a large quantity of titanium oxide, in the case of the higher fluence, followed by annealing at 1200°C. Since the toughness of TiO₂ is higher than that of alumina, it is normal that the toughness increases with annealing temperature. At a certain temperature the oxide layer disappears from the implanted layer, which in the present case takes place at 1500°C. Most previous work has been carried out in single crystal alumina and the present work confirms that previous knowledge is equally applicable to polycrystalline aluminas.

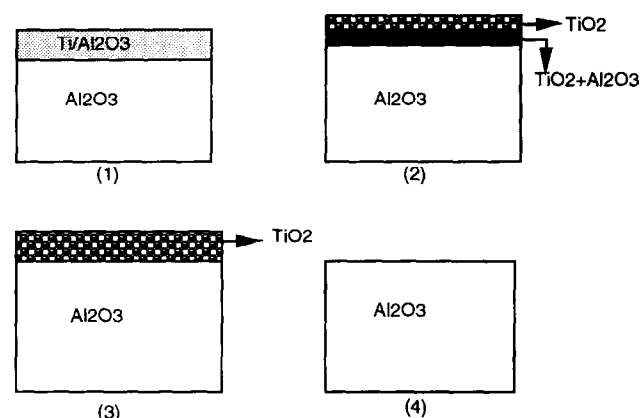


Fig. 9. Schematic representation of the evolution of implanted layer (1) Room-T (2) 1000°C (3) 1200°C (4) 1500°C.

It can therefore, depending on the desired applications, either increase the hardness by implantation, or the toughness by a combination of implantation doses followed by annealing at an optimum temperature. In the last case there is a great possibility of the creation of a third phase. Thus the surface could be suitably treated to obtain surface layers favourable for tribological application.

Acknowledgements

The authors wish to express thanks to the Direction Recherche Etudes et Techniques for their financial help, in the form of a research contract, the Groupe de Traitement de Surface, Institut de Physique Nucléaire de Lyon for ion implantation and to the Laboratoire Métallurgie et Physique des Matériaux de L'Ecole Centrale de Lyon for the X-ray analyses.

References

1. McHargue, C. J., Farlow, G. C., White, C. W., Williams, J. M., Appleton, J. M. & Naramoto, H., The amorphisation of the ceramics by ion beams. *Mater. Sci. Eng.*, **69** (1985) 123–7.
2. Bull, S. J. & Page, T. F., Thermal effects on the microstructure and mechanical properties of ion implanted ceramics. *J. Mater. Sci.*, **26** (1991) 3086–106.
3. Bull, S. J. & Page, T. F., The friction and wear of ion-implanted ceramics: the role of adhesion. *Nucl. Ins. Meth.*, North-Holland, **B32** (1988) 91–5.
4. Paletto, S., Moutel, A. & Fantozzi, G., *Annealing effects on mechanical properties of implanted alumina and zirconia*. SMT 4, Paris (1990).
5. McHargue, C. J., Appleton, B. R. & White, C. W., Structure property relationships in ion implanted ceramics. NATO, Les Arcs France (1983).
6. Burnett, P. J. & Page, T. F., An investigation of ion implantation induced near surface stresses and their effects in sapphire and glass. *J. Mater. Res.*, **20** (1985) 4624–46.
7. McCallum, J. C., White, C. W., Sklad, P. S. & McHargue, C. J., Annealing environment effect in solid-phase epitaxial regrowth of Fe-implanted Al_2O_3 . *Nucl. Ins. Meth.*, North-Holland, **B46** (1990) 137–43.
8. Donnet, C., Caractérisation physico-chimique de céramiques thermomécaniques traitées par implantation ionique. PhD thesis, University of Claude Bernard Lyon 1, France, 1990.
9. Liang, K. M., Torecillas, R., Orange, G. & Fantozzi, G., Evaluation by indentation of fracture toughness in ceramics. *J. Mater. Sci.*, **25** (1990) 207–14.
10. McHargue, C. J., The mechanical properties of ion implanted ceramics: a review. *Defect and Diffusion Forum*, **57–58** (1988) 359–80.
11. Bourdillon, A. J., Bull, S. J., Burnett, P. J. & Page, T. F., The charge state of Ti ions implanted into sapphire: an EXAFS study. *J. Mater. Sci.*, **21** (1986) 1547–52.
12. McHargue, C. J., Structure and mechanical properties of ion implanted ceramics, *Nucl. Ins and Meth. in Phys. Res.*, North-Holland, **B19** (1987) 171–5.
13. O'Hern, M. E., McHargue, C. J., White, C. W. & Farlow, G. C., The effect of chromium implantation on the hardness, elastic modulus, and residual stress of Al_2O_3 . *Nucl. Ins. Meth.*, North-Holland, **B46** (1990) 171–5.
14. Lawn, B. R. & Fuller, E. R., Measurement of thin-layer surface stresses by indentation fracture. *J. Mater. Sci.*, **19** (1984) 4061–7.
15. Kreft, G. B. & Eernisse, E. P., Volume expansion and annealing compaction of ion bombarded single-crystal and polycrystalline $\alpha\text{-Al}_2\text{O}_3$. *J. Appl. Phys.*, **49** (1978) 2725–30.